The Staphylococcal α-Toxin Pore Has a Flexible Conformation†

Beatrix Vécsey-Semjén,‡,§ Stefan Knapp,|| Roland Möllby,‡ and F. Gisou van der Goot*,§

Microbiology and Tumorbiology Center, Karolinska Institutet, 17177 Stockholm, Sweden, Center for Structural Biochemistry, Karolinska Institutet, NOVUM, 14157 Stockholm, Sweden, and Département de Biochimie, Université de Genève, 30 quai E. Ansermet, 1211 Genève 4, Switzerland

Received October 15, 1998; Revised Manuscript Received January 26, 1999

ABSTRACT: The α-toxin from *Staphylococcus aureus* undergoes several conformational changes from the time it is released from the bacterium to the moment it forms a channel in the plasma membrane of its target cell. It is initially a soluble monomer, which undergoes membrane binding and oligomerization into a heptameric ring and finally inserts into the lipid bilayer to form a pore. Here we have analyzed the stability of different forms of the α-toxin (monomer as well as heptamers in solution, bound to the membrane and membrane-inserted) by differential scanning calorimetry and limited proteolysis. Data presented here show that, in contrast to both the membrane-bound prepore complex and the monomer in solution, the membrane-inserted α-toxin channel does not undergo cooperative unfolding and is highly susceptible to proteases. These observations suggest that the channel has a looser conformation. Interestingly, resistance to proteases could be recovered upon solubilization of the channel, indicating that the loss of rigid tertiary packing only occurred upon membrane insertion. Far-UV CD data, however, suggest that the transmembrane β-barrel must be stably folded and that therefore only the Cap and Rim domains of the channel are loosely packed. All together, our data show that the α-toxin channel is not a rigid complex within the membrane but adopts a rather flexible conformation.

α-Toxin is secreted by *Staphylococcus aureus* as a water-soluble, 33 kDa single-chain, active polypeptide (for reviews, see refs *1*−*3*). After binding to the target cell surface has occurred, possibly via specific receptor molecules, collision between toxin monomers at the membrane surface leads to the formation of a stable heptameric complex (*4*, *5*). This complex is initially nonlytic. α-Toxin can be blocked in a membrane-bound, nonlytic conformation by introducing point mutations (*6*−*8*) or by manipulating parameters such as pH and lipid composition (*9*). It has also been proposed that this nonlytic complex exists in vivo at the surface of α-toxin insensitive cells (*10*). A subsequent prepore to pore transition is required for channel formation. This transition involves membrane insertion of the central, glycine-rich, loop (*11*, *12*). The loops from the seven subunits of the complex then come together and form a 14-stranded transmembrane β-barrel (*9*) as beautifully illustrated by the X-ray structure of the heptamer in the presence of detergent (*5*; also see Figure 5).

Each step in the mechanism of action, i.e., membrane binding, heptamerization, and membrane insertion, involves conformational changes not only of quaternary structure but also of tertiary and secondary structures. The changes in structure that take place have not been precisely characterized; however, the following observations have been made. Upon membrane binding and oligomerization, tryptophan residues that are initially buried in the soluble structure become accessible to soluble quenchers, indicating a change in the tertiary packing (*9*). The structure, however, remains rigid as witnessed by the presence of a well-defined near-ultraviolet circular dichroism (UV CD)[1] signal (*9*) and a lack of protease sensitivity except for the N-terminal latch (*7*). Even the central loop, which is very sensitive to proteases in the soluble form (*13*−*15*), becomes protected (*6*, *7*, *13*). Upon subsequent membrane insertion, an increase in the level of β-sheet structure was observed, most likely corresponding to the folding of the central loops into a β-barrel (*9*) which penetrates into the bilayer (*7*, *11*, *15*−*18*). In this membrane-inserted conformation, tryptophan residues are no longer accessible to soluble quenchers but become accessible to quenching by bromide attached in the middle of the acyl chain of the lipid (*9*). The recently determined structure of the heptamer (*5*) indeed reveals that many tryptophans are close to the acyl chain−headgroup interface. Also after membrane insertion, the aromatic residues are free to rotate as witnessed by the collapse of the near-UV CD signal (*9*). This latter observation raises the possibility that the membrane-inserted toxin is not a rigid complex but rather that it has a loose conformation.

In this paper, we have probed the conformation of the α-toxin channel by differential scanning calorimetry, binding of the hydrophobic dye bis-ANS, and limited proteolysis.

† This work has been supported by a grant from the Swiss National Science Foundation to F.G.v.d.G. and the Karolinska Institutet's fonder to R.M.

* Corresponding author. Telephone and fax: (41) 22 702 6414. E-mail: Gisou.vandergoot@biochem.unige.ch.

‡ Microbiology and Tumorbiology Center, Karolinska Institutet.

§ Université de Genève.

|| Center for Structural Biochemistry, Karolinska Institutet.

[1] Abbreviations: DOPG, dioleoylphosphatidylglycerol; DOPC, dioleoylphosphatidylcholine; HEPES, *N*-(2-hydroxyethyl)piperazine-*N*′-2-ethanesulfonic acid; UV CD, ultraviolet circular dichroism.

10.1021/bi982472k CCC: $18.00
Published on Web 03/18/1999

We found that within the membrane environment, but no longer upon solubilization with detergents, most of the α-toxin channel, with the probable exception of the transmembrane β-barrel, has loose tertiary packing.

EXPERIMENTAL PROCEDURES

Protein Purification. α-Toxin was produced by *S. aureus* strain Wood 46 and purified as previously described (*19*). The protein concentration was determined by measuring the absorption at 280 nm based on an OD of 1.8 for a 1 mg/mL solution (*20*).

Preparation of Liposomes. Liposomes were formed of either pure dioleoylphosphatidylglycerol (DOPG) or of a 1:1 mixture of DOPG and dioleoylphosphatidylcholine (DOPC) (Avanti Polar Lipids, Alabaster, AL). Small unilamellar vesicles were prepared by sonication as previously described (*21*) in 20 mM MES and 150 mM NaCl at pH 4.75 and 5 for DOPG and DOPC/DOPG (50:50, w:w), respectively. α-Toxin (10 μM) was added to the vesicles (7.5 mM lipids) and the mixture incubated for 60 min at room temperature.

Differential Scanning Calorimetry. All calorimetric scans were performed using a MicroCal MCS calorimeter at a scanning rate of 60 °C/h. The calorimeter was controlled by the MCS OBSERVER program (MicroCal). For monomeric α-toxin in solution, the sample was dialyzed at 4 °C against the buffer used during measurements. Measurements at pH 7 were performed in a buffer containing 150 mM NaCl and 20 mM Na_2HPO_4/citric acid. The pH of the buffers (between 7 and 3.8) was not significantly affected by temperature between 15 and 65 °C. The samples were degassed for 5 min before calorimetric analysis. A prescan up to 25 °C (during which no transitions were observed) was carried out before each scan to improve the baseline stability. Buffer baselines were measured under identical conditions and subtracted from the corresponding scan. When measurements were performed in the presence of lipid vesicles, the reference cell contained protein-free vesicles in the corresponding buffer. The toxin concentration was 1−1.2 mg/mL in the absence of liposomes and 0.5−0.7 mg/mL in the presence of liposomes.

Bis-ANS Binding Level as a Function of Temperature. The binding level of bis-anilino-naphthalene sulfonate (bis-ANS, Molecular Probes) was measured as previously described (*22*) using a PTI spectrofluorometer equipped with a thermostated cell holder. The excitation and emission wavelengths were 380 and 480 nm, respectively, and the excitation and emission spectral bandwidths were 2 and 3 nm, respectively. Measurements were performed while the mixture was being stirred constantly. The temperature was raised at a speed of 0.7 °C/min. The final bis-ANS concentration was 3.7 μM. α-Toxin in the presence of DOPG or DOPC/POPG vesicles was prepared as described above. The final α-toxin concentration was always 0.48 μM. For each protein scan, the scan for the corresponding buffer containing lipids (except for α-toxin in solution) and bis-ANS was subtracted.

Limited Proteolysis. All protease treatments were performed for 40 min at 37 °C. Digests were stopped by adding PMSF to a final concentration of 1 mM. Monomeric α-toxin was treated in 20 mM Na_2HPO_4/citric acid and 150 mM NaCl at the desired pH. The prepore α-toxin obtained in the presence of DOPC/DOPG (50:50) vesicles and the α-toxin inserted in DOPG vesicles were treated in 20 mM MES and 150 mM NaCl at pH 5.0 and 4.75, respectively. Treatments with trypsin and proteinase K were performed at a 1:50 enzyme:protein molar ratio and those with Pronase at a 1:100 protein:protein ratio (w:w). To compensate for the pH-induced loss of activity of trypsin, digests were performed at a 1:5 protein:protease molar ratio at pH 3.6. Samples containing liposomes were delipidated by methanol/chloroform extraction before resolubilization in sample buffer and analyzed by SDS−PAGE (*23*). All samples were heated to 80 °C for 5 min prior to gel loading.

N-Terminal Sequence Analysis. Sequence analyses were carried out on an Applied Biosystems (Foster City, CA) 477A pulsed liquid phase sequencer with an on line PTH 120A analyzer. Cycle programs were adapted to our reaction carriages. Chemicals were purchased from the manufacturer. The protein samples were separated by SDS−PAGE and transferred to poly(vinylidene difluoride) (PVDF) membranes (Immobilon-P^{sq} Transfer Membrane, Millipore). The PVDF membranes were stained with Coomassie Brilliant Blue (*24*). The initial yield was 47%, calculated from a sequenced β-lactoglobulin standard. Repetitive yields were 97−97.5%.

RESULTS

In contrast to the native soluble form of α-toxin and the membrane-bound prepore, the α-toxin channel does not give rise to any CD signal in the near-UV spectral region and exposes multiple protease cleavage sites (*9*). On the basis of these findings, we have hypothesized that the α-toxin channel might have a rather loose conformation in the membrane environment. Here, we investigated this possibility by probing the conformation of the α-toxin channel by differential scanning calorimetry (DSC) and limited proteolysis and compared it to that of three other forms of toxin, i.e., the native soluble form, the membrane-bound prepore, and the acid-induced molten globule state. This latter conformation was studied because our previous data strongly suggested that partial unfolding of α-toxin is required and is a rate-limiting step in the channel formation process (*9*). We indeed observed that the rate of membrane insertion correlated with the appearance of this folding intermediate (*22*).

Thermal Unfolding of Monomeric α-Toxin. The thermal unfolding of monomeric α-toxin was studied using differential scanning calorimetry (DSC) at different pH values ($3.7 < pH < 7$). Thermal unfolding of α-toxin was irreversible presumably due to the observed post-transitional aggregation of the protein. This irreversibility unfortunately hinders thermodynamic analysis of the calorimetric data. However, since the measured calorimetric endotherms were symmetrical and apparently not disturbed by the post-transitional aggregation, the melting temperature of the protein (T_m) could be determined with a reasonable accuracy (Figure 1).

At pH 7, α-toxin melted at 55 °C. The melting temperature gradually decreased at acidic pH, with a concomitant broadening of the spectrum, reaching 42 °C at pH 4.5 (Figure 1B). Upon further acidification (pH 3.8), the calorimetric endotherm was considerably broadened (Figure 1A), indicating a lack of cooperativity for the melting process. Finally, no calorimetric transitions could be observed at pH ≤3.7.

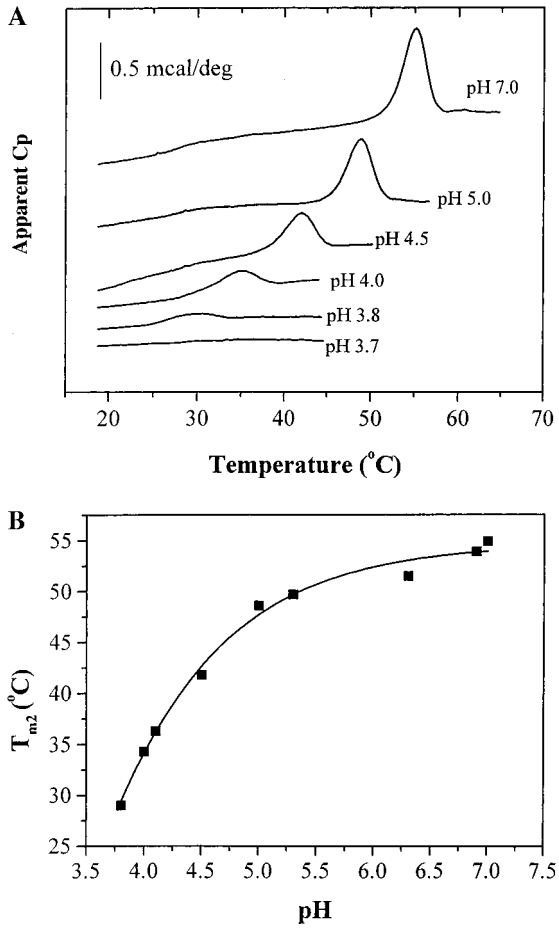

FIGURE 1: pH dependence of the thermal unfolding of α-toxin. (A) DSC endotherms of monomeric α-toxin (1 mg/mL) were measured at different pH values in buffers containing 20 mM Na_2HPO_4/citric acid and 150 mM NaCl. Shown are raw data after subtraction of the corresponding buffer baselines. (B) The calorimetrically determined melting temperature (T_m) of monomeric α-toxin plotted as a function of pH.

The lack of thermal unfolding of α-toxin at pH 3.7 is in agreement with our previous observations that the toxin adopts a molten globule-like configuration at this pH value (*22*). It is interesting to note that, using spectroscopic methods, we could not detect any unfolding down to pH 4 (*22*). Therefore, it appears that between pH 4 and 6, acidification leads to destabilization of α-toxin, as indicated by a decrease in the melting temperature, but does not yet trigger physical unfolding, which would only occur at more acidic pHs. Similar observations have been made previously by Muga et al. for the pore-forming domain of colicin A (*25*). These authors argue rightly that "substantial destabilization can occur at a pH 1 unit higher than that required for spectroscopically detectable transition to a molten globule state" and that "further loosening of the partly destabilized but still native like structure could be facilitated by factors other that local acidity" near the membrane surface. We believe the same reasoning can be applied to α-toxin.

Unfolding of the Membrane-Bound and Membrane-Inserted α-Toxin Heptamer. We next studied the thermal stability of the α-toxin associated with membranes both as a nonlytic prepore and as a membrane-inserted channel. We have previously established that α-toxin is trapped in the membrane-bound prepore state in the presence of DOPC/DOPG (50:50) vesicles at pH 5.0 but proceeds to the channel

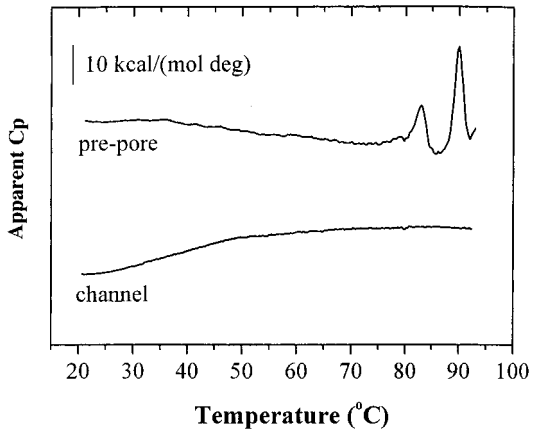

FIGURE 2: DSC thermograms for the membrane-bound prepore and the membrane-inserted channel of α-toxin. DSC thermogram of α-toxin either in the presence of DOPC/DOPG vesicles at pH 5.0 (prepore stage, 0.6 mg/mL) or in the presence of DOPG vesicles at pH 4.75 (channel form, 0.6 mg/mL). Note that under both conditions, the toxin is heptameric (*9*). In these experiments, the reference cell contained the corresponding toxin-free vesicles in buffer. Shown are raw data after subtraction of the corresponding baselines and after concentration normalization. Buffers contained 150 mM NaCl and 20 mM MES/Na.

form in the presence of DOPG vesicles at pH 4.75 (*9*). These conditions were used for the present DSC experiments. The thermograms of these two forms of the toxin were strikingly different (Figure 2). At least two thermal transitions, at 83 and 90 °C, were observed for the membrane-bound prepore. To what these melting events correspond is not clear. They could represent melting of two domains. Alternatively, one event could correspond to subunit dissociation (since the α-toxin heptamer is known to be heat sensitive) and the other to monomer unfolding.

In contrast to the prepore, no transition was detected for the α-toxin channel up to 95 °C (Figure 2). This observation suggests either that the channel is more stable then any of the other forms of the toxin or that it has undergone noncooperative unfolding over a broad temperature range. The former possibility seems unlikely in light of our previous observations that the channel form showed no near-UV CD signal and that the form also has an increased susceptibility to proteases. The lack of thermal unfolding upon membrane insertion however is reminiscent of other pore-forming toxins for colicin A (*25*), the δ-endotoxin cytA (*26*), and *Escherichia coli* hemolysin (*27*). To verify that the conformation of the α-toxin channel was sensitive to temperature, we measured the binding of the hydrophobic dye bis-ANS as a function of temperature. As shown in Figure 3, binding of bis-ANS to the channel form was far more pronounced then binding to the prepore, further confirming the partly unfolded conformation of the membrane-inserted complex. As the temperature increases, the level of binding of bis-ANS gradually decreased, suggesting unfolding of the protein. As expected, the level of binding of bis-ANS to the prepore was low and did not change with temperature up to 60 °C. In the inset, the level of binding of bis-ANS to α-toxin in solution at pH 4.75 as a function of temperature is shown. The maximal fluorescence at 42 °C is in good agreement with the unfolding analyzed by DSC (Figure 1B).

These observations show that the heptamer in solution or bound to membranes in a nonlytic form undergoes well-

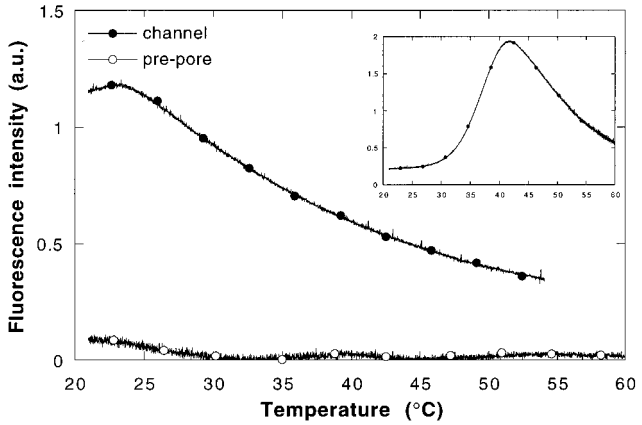

FIGURE 3: Binding of bis-ANS to the different forms of α-toxin as a function of temperature. The fluorescence of bis-ANS (3.7 μM) in the presence of the α-toxin prepore (DOPC/DOPG vesicles at pH 5.0) or the channel (DOPG vesicles at pH 4.75) was measured as a function of temperature. The fluorescence of bis-ANS in the presence of the corresponding vesicles in a toxin-free medium was subtracted for each temperature. In the inset, the fluorescence of bis-ANS (3.7 μM) in the presence of the α-toxin in solution at pH 4.75 (150 mM NaCl and 20 mM Na_2HPO_4/citric acid) was measured as a function of temperature. The fluorescence of bis-ANS in the absence of protein was subtracted. The fluorescence of bis-ANS was not sensitive to temperature in the 20−60 °C range.

defined thermal transitions. However, upon channel formation, cooperative thermal unfolding was no longer observed, suggesting that the protein does not have a tightly packed core. The well-defined far-UV CD spectrum of the channel, which showed an increase in β-sheet content when compared to the prepore (*9*), suggests that the transmembrane barrel has a stable conformation. Therefore, only the Cap and Rim domains of the channel, which composed more than 90% of the complex, would become flexible upon membrane insertion.

Limited Proteolysis of α-Toxin. The conformation of α-toxin in its various forms was additionally probed by limited proteolysis. As shown in Figure 4A, trypsin or proteinase K treatment at pH 5 led to the appearance of a double band with an apparent molecular mass of approximately 17 kDa (lanes 2 and 4) corresponding to nicking in the glycine-rich loop (*13*−*15*). At pH 3.6, however, cleavage occurred at multiple sites as can clearly be seen upon proteinase K treatment (Figure 4A, lane 5). In the heptameric prepore configuration however (lanes 6 and 7), the protein was rather insensitive to protease treatment. In contrast in the transmembrane form (lanes 8 and 9), the protein was highly sensitive to proteolytic degradation. These observations are in full agreement with our previous limited proteolysis studies using trypsin (*9*). All these limited proteolysis studies show that (i) the native monomer is nicked by proteases only in the middle of the polypeptide chain, (ii) the acid-induced molten globule (pH 3.6) is far more sensitive to proteases, thereby leading to a number of different fragments, (iii) the membrane-bound prepore complex is not sensitive to proteases, and finally (iv) the α-toxin channel is highly protease sensitive.

The high protease sensitivity of the α-toxin channel (Figure 4), the lack of a thermal transition observed in the DSC experiments (Figure 2), the ability to bind bis-ANS (Figure 3), and our previous observation that the channel does not exhibit any near-UV CD signal (*9*) clearly indicate that the

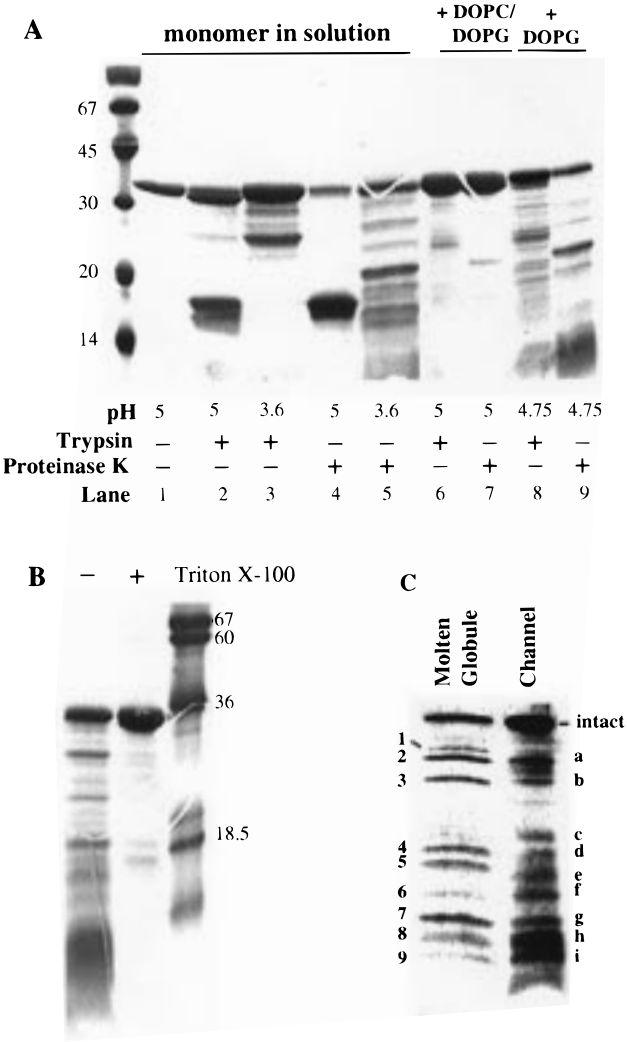

FIGURE 4: SDS−PAGE of proteolytic fragments of α-toxin monomers, membrane-bound prepores, and channels. (A) Coomassie Brilliant Blue-stained SDS−PAGE of the α-toxin monomer, the membrane-bound prepore complex (in the presence of DOPC/DOPG vesicles at pH 5; see the text), and the transmembrane channel (in the presence of DOPG vesicles at pH 4.75) treated with trypsin (1:50 protease:protein molar ratio) or proteinase K (1:50 protease:protein molar ratio) for 40 min at 37 °C. (B) Coomassie Brilliant Blue-stained SDS−PAGE of the membrane-inserted α-toxin channel treated with Pronase (1:100 protease:protein molar ratio) in the presence or absence of 1% Triton X-100. (C) Coomassie Brilliant Blue-stained PVDF membrane used for sequencing analysis. Shown are proteolytic fragments of the Pronase-treated acid-induced molten globule state of α-toxin (pH 3.6) and the Pronase-treated α-toxin channel form.

α-toxin channel has a loosened conformation when compared to that of the membrane-bound prepore or the soluble toxin. We investigated whether this conformation was retained upon solubilization of the lipid membrane with the nonionic detergent Triton X-100. Interestingly, the protease sensitivity of the α-toxin channel was dramatically reduced, if not abolished, in the presence of Triton X-100 (Figure 4B, the lack of an effect of Pronase was not due to protease inactivation by Triton X-100 since cleavage of the molten globule form was not affected by the detergent). This is in agreement with our observation that detergent treatment of the transmembrane channel leads to significant recovery of the near-UV CD signal (*9*). Together, these observations indicate that upon detergent solubilization, the α-toxin

Table 1: N-Terminal Sequences of Pronase Cleavage Fragments[a]

molten globule			channel			apparent molecular mass (kDa)
band	N-terminal sequence	starting amino acid	band	N-terminal sequence	starting amino acid	
1	ADSDI	1				29
2	ADSDI	1	a	ADSDI	1	27.5
	SEEGA	69		SEEGA	69	
3	ADSDI	1	b	ADSDI	1	23
			c	ADSDI		18.5
4	DSDIN	2	d	ADSDI	1	18
				SPDFA	225	
5	ADSDI	1				16.5
	KYVGP	147				
			e	nd		
6	nd		f	ADSDI	1	14.5
				SPDFA	225	
7	MKTRN	197	g	nd		13
8	ADSDI	1	h	nd		12.5
	MKTRN	197				
9	ADSDI	1	i	nd		11.5
	MKTRN	197				
	KASKQ	237				

[a] α-Toxin was treated with Pronase (1:100 protease:protein molar ratio, w:w) for 40 min at 37 °C in the soluble monomeric form at pH 3.6 and in the channel form (in the presence of DOPG vesicles at pH 4.75). Fragments were separated by SDS−PAGE and transferred onto a PVDF membrane for N-terminal sequencing. nd, not determined.

heptamer adopts a more tightly packed conformation than it had within the lipid environment and also provides an explanation about why the α-toxin heptamer, with its folded β-barrel, was able to form crystals in the presence of detergent (*5*). These findings also show that the flexible conformation is only adopted when the channel is membrane-inserted.

Characterization of the Proteolytic Fragments. To further characterize the conformation of the α-toxin channel, the cleavage pattern obtained after Pronase treatment was analyzed in more detail. First, the cleavage pattern was not significantly modified when increasing the cleavage time from 15 min to 2 h (not shown), suggesting that once the initial cleavages occurred, the protein remained rather resistant to further proteolysis, suggesting that it was still predominantly folded. Analysis of the cleavage pattern also showed that the fragments obtained from the α-toxin channel had a migration pattern strikingly similar, although not identical, to that obtained upon cleavage of the monomer in the acid-induced molten globule state (Figure 4C), suggesting that the two forms of the protein exposed certain common sites. These observations suggest that the overall tertiary fold of the monomer and that of the heptamer are similar and that oligomerization would only require a minimal change in structure. The only possible difference between the monomer and the heptamer would be the structure and the positioning of the central glycine-rich loop. This is reminiscent of the observations of Petosa et al. (*28*), who have found, on the basis of crystallographic data, that heptamer formation by the protective antigen of anthrax involved only very minor structural changes when compared to the monomer.

The N-termini of several of the fragments shown in Figure 4C were sequenced, and the results are summarized in Table 1. Most fragments had the same N-terminus as full-length α-toxin; however, several new N-termini were identified.

In the acid-induced molten globule state (Figure 4C and Table 1), cleavage occurred at the amino sides of Asp-2 (band 4), Ser-69 (band 2), Lys-147 (band 5), Met-197 (bands 7−9), and Lys-237 (band 9). Since the crystal structure of the α-toxin monomer has not yet been determined, the sites were mapped, for convenience, on the structure of a protomer of the heptamer crystallized in the presence of *n*-octyl β-glucoside (*5*) (Figure 5A). The sites were not clustered in a specific region of the molecule but scattered throughout the three domains, which in the heptamer have been termed the Cap, Rim, and Stem domains. Two sites were found at the top of the Cap domain: after the N-terminal amino acid (Asp-2) and in the loop between strands β13 and β14 (Lys-237). Two other sites were located at the bottom of the Rim domain: within strand β4 (Ser-69) and in the loop between strand β12 and the short B helix (Met-197). The last N-terminus was found at the end of the segment forming the Stem domain (Lys-147).

This latter cleavage site was not found in the channel form as expected since the Stem domain should be protected from proteolysis by the lipid bilayer. However, cleavage at the amino side of Ser-69, at the bottom of the Rim domain, was observed. Bands g−i were not sequenced; however, the comparison of the two lanes in Figure 4C suggests that they might correspond to bands 7−9 and therefore that also in the channel form, cleavage occurs at the amino side of Met-197 at the bottom of the Rim domain (Figure 5). More importantly, two fragments starting at Ser-225 were identified, indicating that cleavage had occurred between helix D and strand β13, i.e., between the Cap and Rim domains (Figure 5). According to the space-filled models of the channel in the presence of detergents shown in Figure 5, Ser-225 is not accessible from outside the complex and is only slightly surface-exposed toward the interior of the ring. The accessibility of this site to Pronase strongly suggests that membrane insertion triggered a conformational change leading to the opening, at least transiently, of a cleft between the Cap and Rim domains that would allow access to the protease. The exposure of hidden sites further supports the view of loose tertiary packing of the Cap and Rim domains when the channel is membrane-inserted.

DISCUSSION

In this work, we demonstrated by combining differential calorimetry, fluorescence spectroscopy, and limited proteolysis that α-toxin adopts in its lytic membrane-imbedded form a conformation more flexible and protease sensitive than the membrane-bound prepore complex or the monomer in solution. This conclusion is based on the observations that the α-toxin channel exhibits no well-defined thermal unfolding (Figure 2), does not give rise to any CD signal in the near-UV spectral region (*9*), is able to bind the hydrophobic dye bis-ANS (Figure 3), and is very sensitive to a variety of proteases (Figure 4). In particular, a proteolytic site that is predicted to be hidden in the complex that was crystallized in the presence of detergents (Figure 4) was found to be accessible. The membrane-imbedded channel is however still folded to a large extent as indicated by the well-defined far-UV CD spectrum (*9*) and the observation that after the initial protease cleavages have occurred, the protein remains resistant to further degradation. It appears that the transmembrane β-barrel must have a rather rigid structure but that the Cap and Rim domains are more loosely packed. It has been observed, in a similar manner, that the pore-forming

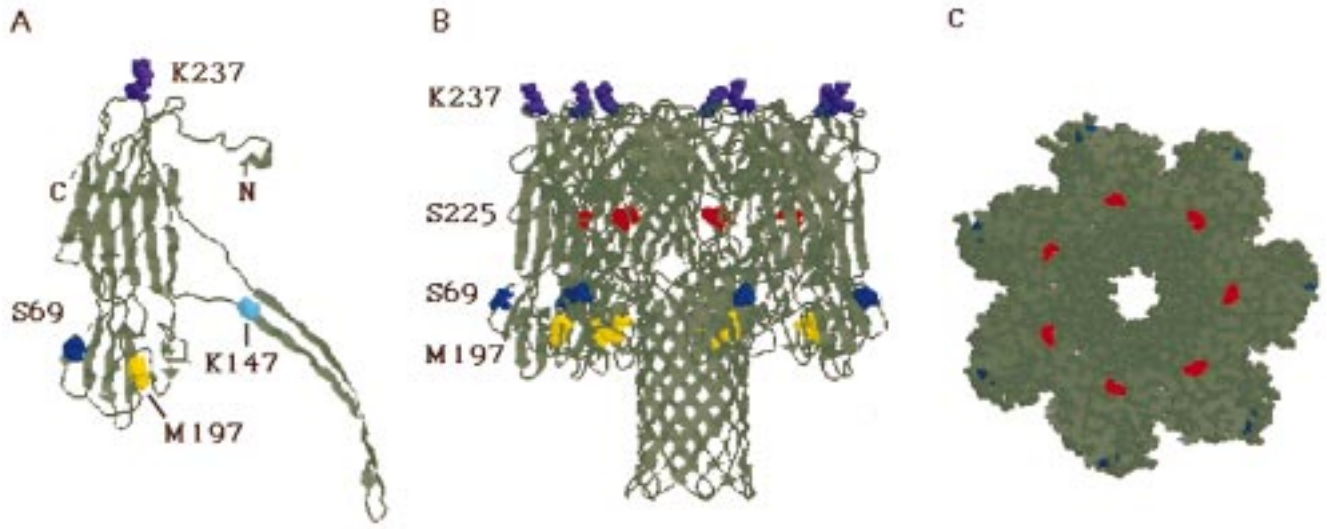

FIGURE 5: Mapping of the Pronase cleavage site. **(**A) Ribbon diagram of an α-toxin protomer based on the crystal structure of the heptamer obtained in detergent (*5*). Pronase treatment of the acid-induced molten globule state led to at least four new N-termini cleavage sites (see Table 1 and Figure 4C): Ser-69 (blue), Lys-147 (light blue), Met-197 (yellow), and Lys-237 (purple). Although the structure of the α-toxin monomer in solution at acidic pH might be somewhat different from that of a protomer in the detergent-solubilized heptamer, the amino acids corresponding to the new N-termini were mapped and are shown as space-filled diagrams. (B) Ribbon diagram of a side view the α-toxin heptamer in the presence of detergents (*5*). Pronase treatment of the α-toxin channel in DOPG vesicles led to a variety of fragments, one of which was a fragment starting at amino acid Ser-225 (red). (C) The portion of the channel situated above Ser-225 (red) in panel B was removed, and a space-filled diagram of a top view of the remaining structure is shown. Ser-225 is not accessible from outside the channel but is somewhat surface-exposed toward the lumen of the heptameric ring. The diameter of the lumen at the top of the channel is 25 Å, which appears to be too small to allow the passage of a protease. Ser-69 is blue.

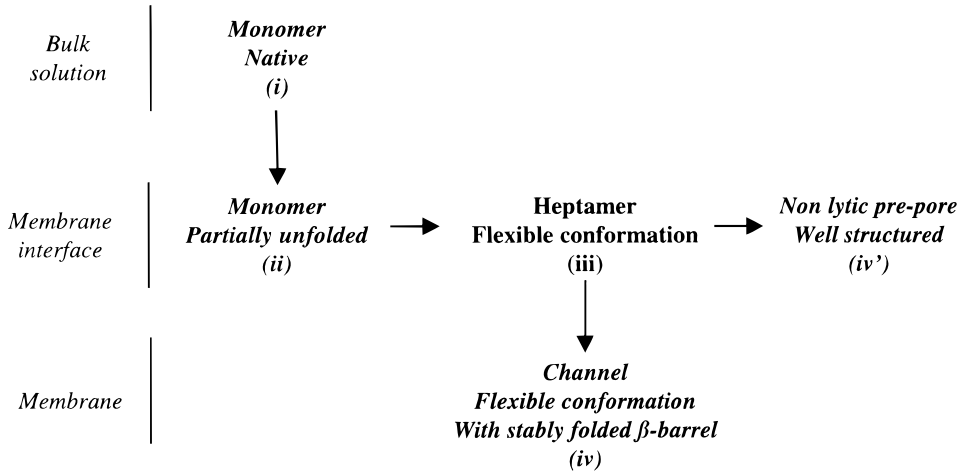

FIGURE 6: Hypothetical mode of action of α-toxin. On the basis of our present and previous observations and on data from the literature, we propose the following steps toward channel formation of α-toxin. The toxin is secreted by the bacterium as a monomer with a tight tertiary packing (i). At the membrane interface due to a low pH or another trigger that remains to be identified, the toxin would partially unfold (ii). This folding intermediate would be competent to oligomerize into a heptameric ring. We speculate that the heptamer is initially in a flexible conformation (iii) that is competent for membrane insertion (iv), thereby leading to a channel which is also partly flexible. The flexible heptamer could also proceed toward the formation of a nonlytic membrane-bound complex (iv′) which would no longer be membrane insertion competent. This latter configuration of the toxin would correspond to what others and we have termed the prepore. The conformations denoted in bold italics have already been visualized and characterized (i, ii, iv, and iv′); the flexible heptamer is hypothetical (iii).

domains of colicins A and E1 (*25*, *29*, *30*), the δ-endotoxin cytA (*26*), and *E. coli* hemolysin (*27*) have a flexible conformation when they are membrane-inserted. Importantly, the flexible conformation of the α-toxin channel was only encountered in the membrane environment since solubilization of the channel in detergent led to a loss of protease sensitivity (Figure 4B) and a significant recovery of the near-UV CD signal (*9*). In the presence of detergent, the α-toxin heptamer recovered rigid tertiary packing.

Our previous work indicated that partial unfolding of α-toxin is required for channel formation to occur (*22*). Here we show that the final channel has a more flexible conformation with the probable exception of the transmembrane β-barrel. Combined, these observations suggest that the nonlytic heptameric intermediate must also have a flexible conformation and that the rigid membrane-bound complex we and others have characterized and called the prepore is in fact a side track of the channel formation pathway. We therefore proposed the following speculative model for the channel formation process of α-toxin (Figure 6). The toxin is secreted by the bacterium as a monomer with a rigid tertiary structure (i) as indicated by the presence of a well-defined near-UV CD spectrum and a maximum emission wavelength of tryptophan residues of 331 nm (*13*, *22*, *31*).

In the membrane vicinity, a low pH or other factors that remain to be identified would trigger partial unfolding (ii) (*22*). This unfolding intermediate would be competent for oligomerization, provided the toxin concentration is high enough, thereby leading to a heptameric complex. We speculate that the heptamer is initially and transiently in a flexible conformation (iii). This flexible heptameric intermediate, which has at present never been visualized presumably because it is very short-lived, could either evolve toward a stable nonlytic membrane-bound complex (iv′) or insert into the membrane and form the channel (iv). In this channel form, the Cap domain of the channel would have a flexible conformation while the transmembrane β-barrel would probably have a stable structure. The stable nonlytic complex (iv′) would correspond to what others and we have termed the prepore. Certain point mutations (*32*, *33*) or specific experimental conditions (*9*) would drive the reaction toward the accumulation of prepore, thereby preventing channel formation. In the model proposed here, only the flexible heptameric intermediate would be competent for membrane insertion. A drop in pH or other factors would allow the rigid prepore complex to recover its membrane insertion competence. The challenge for the future will be to determine whether indeed such an intermediate exists and to analyze its properties.

ACKNOWLEDGMENT

We thank Claire Lesieur, Marc Fivaz, and Jean Gruenberg for critical reading of the manuscript. We are very grateful to Eric Gouaux for providing us with the α-toxin coordinates and to Jürgen Engel for giving us free access to his differential scanning calorimeter which enabled us to perform the preliminary experiments for this study.

REFERENCES

1. Bhakdi, S., Bayley, H., Valeva, A., Walev, I., Walker, B., Kehoe, M., and Palmer, M. (1996) *Arch. Microbiol. 165*, 73−79.
2. Lesieur, C., Vecsey-Semjn, B., Abrami, L., Fivaz, M., and van der Goot, F. G. (1997) *Mol. Membr. Biol. 14*, 45−64.
3. Gouaux, E. (1998) *J. Struct. Biol. 121*, 110−122.
4. Gouaux, J. E., Braha, O., Hobaugh, M. H., Song, L., Cheley, S., Shustak, C., and Bayley, H. (1994) *Proc. Natl. Acad. Sci. U.S.A. 91*, 12828−12831.
5. Song, L., Hobaugh, M. R., Shustak, C., Cheley, S., Bayley, H., and Gouaux, J. E. (1996) *Science 274*, 1859−1866.
6. Walker, B., Krishnasastry, M., Zorn, L., and Bayley, H. (1992) *J. Biol. Chem. 267*, 21782−21786.
7. Walker, B., Braha, O., Cheley, S., and Bayley, H. (1995) *Chem. Biol. 2*, 99−105.
8. Fang, Y., Cheley, S., Bayley, H., and Yang, J. (1997) *Biochemistry 36*, 9518−9522.
9. Vecsey-Semjen, B., Lesieur, C., Möllby, R., and van der Goot, F. G. (1997) *J. Biol. Chem. 272*, 5709−5717.
10. Valeva, A., Walev, I., Pinkernell, M., Walker, B., Bayley, H., Palmer, M., and Bhakdi, S. (1997) *Proc. Natl. Acad. Sci. U.S.A. 94*, 11607−11611.
11. Ward, R. J., Palmer, M., Leonard, K., and Bhakdi, S. (1994) *Biochemistry 33*, 7477−7484.
12. Valeva, A., Weisser, A., Walker, B., Kehoe, M., Bayley, H., Bhakdi, S., and Palmer, M. (1996) *EMBO J. 15*, 1857−1864.
13. Tobkes, N., Wallace, B. A., and Bayley, H. (1985) *Biochemistry 24*, 1915−1920.
14. Blomqvist, L., Bergman, T., Thelestam, M., and Jörnvall, H. (1987) *FEBS Lett. 211*, 127−132.
15. Palmer, M., Weller, U., Messner, M., and Bhakdi, S. (1993) *J. Biol. Chem. 268*, 11963−11967.
16. Walker, B., Krishnasastry, M., and Bayley, H. (1993) *J. Biol. Chem. 268*, 5285−5292.
17. Walker, B., Kasianowicz, J., Krishnasastry, M., and Bayley, H. (1994) *Protein Eng. 7*, 655−662.
18. Walker, B., and Bayley, H. (1994) *Protein Eng. 7*, 91−97.
19. Lind, I., Ahnert-Hilger, G., Fuchs, G., and Gratzl, M. (1987) *Anal. Biochem. 164*, 84−89.
20. Moniatte, M., Lesieur, C., Vecsey-Semjen, B., Buckley, J. T., Pattus, F., van der Goot, F. G., and van Dorsselaer, A. (1997) *Int. J. Mass Spectrom. Ion Processes 169/170*, 179−199.
21. van der Goot, F. G., González-Mañas, J. M., Lakey, J. H., and Pattus, F. (1991) *Nature 354*, 408−410.
22. Vecsey-Semjen, B., Möllby, R., and van der Goot, F. G. (1996) *J. Biol. Chem. 271*, 8655−8660.
23. Laemmli, U. K. (1970) *Nature 227*, 680−685.
24. Matsudaira, P. (1987) *J. Biol. Chem. 262*, 10035−10038.
25. Muga, A., Gonzalez, M. J., Lakey, J. H., Pattus, F., and Surewicz, W. K. (1993) *J. Biol. Chem. 268*, 1553−1557.
26. Butko, P., Huang, F., Pusztai-Carey, M., and Surewicz, W. K. (1997) *Biochemistry 36*, 12862−12868.
27. Bakas, L., Veiga, M. P., Soloaga, A., Ostolaza, H., and Goni, F. M. (1998) *Biochim. Biophys. Acta 1368*, 225−234.
28. Petosa, C., Collier, R. J., Klimpel, K. R., Leppla, S. H., and Liddington, R. C. (1997) *Nature 385*, 833−838.
29. Lakey, J. H., Massotte, D., Heitz, F., Dasseux, J. L., Faucon, J. F., Parker, M. W., and Pattus, F. (1991) *Eur. J. Biochem. 196*, 599−607.
30. Zakharov, S. D., Lindeberg, M., Griko, Y., Salamon, Z., Tollin, G., Prendergast, F. G., and Cramer, W. A. (1998) *Proc. Natl. Acad. Sci. U.S.A. 95*, 4282−4287.
31. Ikigai, H., and Nakae, T. (1985) *Biochem. Biophys. Res. Commun. 130*, 175−181.
32. Jursch, R., Hildebrand, A., Hobom, G., Tranum-Jensen, J., Ward, R., Kehoe, M., and Bhakdi, S. (1994) *Infect. Immun. 62*, 2249−2256.
33. Pederzolli, C., Cescatti, L., and Menestrina, G. (1991) *J. Membr. Biol. 119*, 41−52.

BI982472K